

Performance Evaluation of Interpolated Average CT for PET Attenuation Correction in Different Lesion Characteristics

Cobie Y. T. Ho, Tao Sun, Student Member, IEEE, Tung-Hsin Wu and Greta, S. P. Mok, Member, IEEE

Abstract- Previously we demonstrated the effectiveness of the interpolated average CT (IACT) for attenuation correction (AC) in PET in simulations and clinical patients. This study aims to evaluate the performance of IACT for thoracic lesions with different sizes, uptake ratios and locations. The XCAT phantom was used to simulate noisy ^{18}F -FDG distribution based on the clinical count level with respiratory motion amplitude of 2 cm and 3 cm. The average activity and attenuation maps represented static PET and cine average (CACT) respectively. IACT was generated by the end-inspiration and end-expiration phases of the attenuation maps (HCT-in and HCT-ex) using deformable registration method. Spherical 10 mm and 20 mm lesions were simulated at 4 locations individually, including the lower left lung (LLL), lower right lung (LRL), middle right lung (MRL) and upper right lung (URL). Four target-to-background ratios (TBR), including 4:1 and 8:1 for respiratory motion of 2 cm, 6:1 and 12:1 for respiratory motion of 3 cm, were modeled. The noisy sinograms with attenuation modeling were generated and reconstructed with different AC maps by STIR (Software for Tomographic Image Reconstruction), using OS-EM with up to 300 updates. Normalized mean square error (NMSE), mutual information (MI) and TBR were analyzed. The NMSE and MI results showed that PET_{CACT} and PET_{IACT} were more similar to the original phantom as compared to PET_{HCTs} . For TBRs, the differences between CACT/IACT and HCTs AC were more significant for lesions in the lower lung with $\text{PET}_{\text{HCT-ex}}$ showed higher TBR and $\text{PET}_{\text{HCT-in}}$ showed lower TBR as compared to $\text{PET}_{\text{CACT}}/\text{PET}_{\text{IACT}}$ for all lesion sizes, uptake ratios and respiratory motion amplitudes. The TBRs for 10 mm lesion were more difficult to be recovered in all AC schemes. Better lesion localization and more stable quantitation for different lesion characteristics make IACT a good alternate for AC as compared to conventional HCT/CACT.

I. INTRODUCTION

Respiratory motion, the main factor for mis-registration and artifacts in thoracic PET/CT, can cause localization and quantitation errors of tumors. Cine average CT (CACT) for

attenuation correction (AC) in PET was proposed to reduce respiratory artifacts as compared to conventional helical CT (HCT) with concomitant high radiation dose

Previously we proposed an interpolated average CT (IACT) method as a low dose alternate of CACT. The effectiveness of IACT for a range of respiratory motion amplitudes was evaluated in a simulation study [1] and its clinical feasibility was demonstrated [2, 3]. This study aims to evaluate the performance of IACT for thoracic lesions with different sizes, uptake ratios and locations.

II. MATERIALS AND METHODS

We used the digital 4D Extended Cardiac Torso (XCAT) phantom (Fig. 1 a) to simulate a male patient with realistic noisy ^{18}F -FDG activity distribution based on the clinical count level. We used the analytical projector and OS-EM reconstruction algorithm provided by STIR (Software for Tomographic Image Reconstruction), modeling a GE Discovery STE PET scanner.

The respiratory motion amplitudes were 2 cm and 3 cm with a period of 5.9 seconds. The respiratory cycle was divided into 13 phases (Fig. 1 b), starting from the end-inspiration phase. The averages of the 13 phases of the activity and attenuation maps represented static PET and CACT respectively. The end-inspiration and end-expiration phases of the attenuation maps represented 2 HCTs (HCT-in and HCT-ex). B-spline, a deformable image registration algorithm, was used to calculate the deformation vectors which included the lateral, anterior-posterior and inferior-superior displacement for each voxel on two CT volumes based on the Insight Segmentation and Registration Toolkit (ITK). The interpolated phases between 2 extreme phases (HCT-in and HCT-ex) were generated by B-spline combined with an empirical sinusoidal function. The IACT was obtained by averaging the original and interpolated phases.

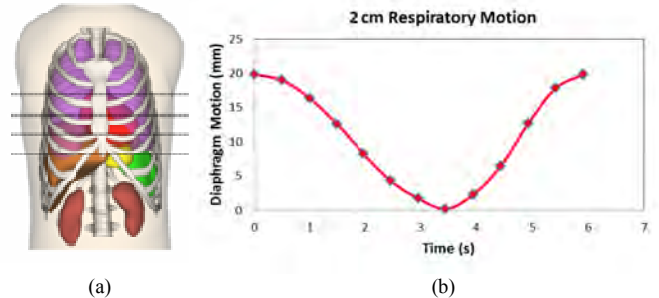


Fig. 1 (a) The XCAT phantom and (b) the respiratory cycle was divided into 13 phases.

Spherical lesions with diameters of 10 mm and 20 mm were simulated at 4 different locations individually, including the lower left lung (LLL), lower right lung (LRL), middle right lung (MRL) and upper right lung (URL) (Fig. 2). Four target-to-background ratios (TBR), including 4:1 and 8:1 for respiratory motion of 2 cm, 6:1 and 12:1 for respiratory motion of 3 cm, were modeled. The noisy sinograms with attenuation modeling were generated and reconstructed with different AC maps (CACT, HCTs and IACTs) (Fig. 3), using OS-EM algorithm with up to 300 updates.

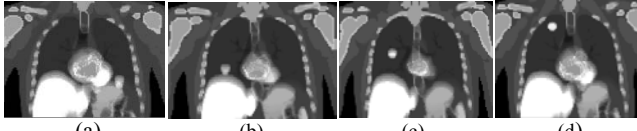


Fig. 2 The noise-free average activity maps with respiratory motion of 2 cm showing the 20 mm thoracic lesion with TBR of 4:1 placed at (a) LLL, (b) LRL, (c) MRL and (d) URL.

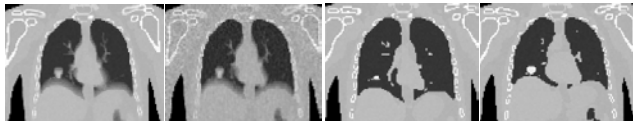


Fig. 3 Sampled mid-coronal slice of different attenuation maps for AC with respiratory motion of 2 cm and 20 mm thoracic lesion placed at LRL.

For reconstructed PET images with no lesions simulated, the following figures-of-merit were analyzed:

(a) Normalized mean square error (NMSE)

The whole PET reconstructed volume using different AC schemes was used to assess the average NMSE as compared to the original phantom.

$$\text{average } NMSE = \frac{1}{n} \sum_{j=1}^n \left(\frac{x_j - \bar{x}_j}{\bar{x}} \right)^2 \quad (1)$$

where n is the number of voxels in the whole reconstructed volume, λ is the voxel count value in the original phantom, $\bar{\lambda}$ is the mean voxel value of the original phantom, x is the voxel count value in the noisy reconstructed images, \bar{x} is the mean voxel value of the reconstructed images and j is the voxel index.

(b) Mutual information (MI)

The MI ($I(X, Y)$) between X and Y , a measure of the statistical dependence between both variables, was applied to estimate the nonlinear image intensity distribution between different PET reconstructed images and the original phantom

$$I(X, Y) = \frac{P(X) + P(Y)}{P(X, Y)} \quad (2)$$

where X and Y are two random variables, i.e., two different images, $P(X)$ is the histogram of X , $P(Y)$ is the histogram of Y and $P(X, Y)$ is the joint histogram of X and Y .

For PET images with lesions, the 2D TBR was calculated from the regions-of-interest (ROIs) drawn on the lesion and the chosen background, based on the central coronal slice of

the PET reconstructed images using different AC maps (Fig. 4):

$$TBR = \frac{\text{Mean}_{\text{hot lesion}}}{\text{Mean}_{\text{background}}} \quad (3)$$

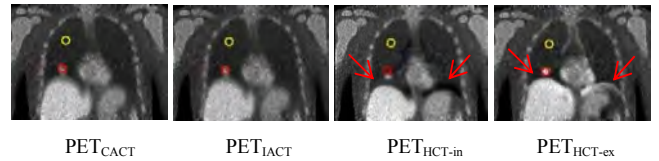


Fig. 4 Sampled PET reconstructed images with AC using different AC maps. Red circles and yellow circles indicated the LRL lesion and background ROIs respectively. Red arrows indicated the misalignment artifacts when using HCTs for AC. Respiratory motion amplitude was 2 cm.

III. RESULTS

For the global image quality indices of NMSE and MI, PET_{IACT} was closer to PET_{CACT} and was superior to that of the PET_{HCTs} (Fig. 5). In Fig. 4, significant artifacts were observed in the regions close to the right and left diaphragm in the PET_{HCTs} , matched with the results of Fig. 5. However, for more local figure-of-merit such as TBR, $\text{PET}_{\text{HCT-ex}}$ showed better performance (Fig. 6-11) as compared to other AC schemes probably because attenuation map of the end-expiration captured the full lesion (Fig. 3) in this case. From visual assessment, the lesion size and shape were similar between PET_{CACT} and PET_{IACT} , while the lesion location deviated for $\text{PET}_{\text{HCT-in}}$. Generally, the TBRs of CACT and IACT were similar for all lesion characteristics, while their differences as compared to the HCTs were more significant for lesions at the lower lung. According to Fig. 6-11, $\text{PET}_{\text{HCT-ex}}$ showed higher TBR and $\text{PET}_{\text{HCT-in}}$ showed lower TBR as compared to $\text{PET}_{\text{CACT}}/\text{PET}_{\text{IACT}}$, and their differences reduced gradually as the lesion moved to the upper locations. Notably, the TBR for the LLL lesion in $\text{PET}_{\text{HCT-ex}}$ was actually overestimated as compared to the truth. It was probably because of the misalignment artifact at the left diaphragm overlaid on the lesion. Similar results were observed in Fig. 6-11 for lesions with different TBRs, lesion sizes and respiratory motion amplitudes. For the lesion size of 10 mm, the TBRs for all cases were smaller than the standard probably because the increased blurring effect when the lesion size was smaller than the respiratory motion amplitude (2 cm and 3 cm).

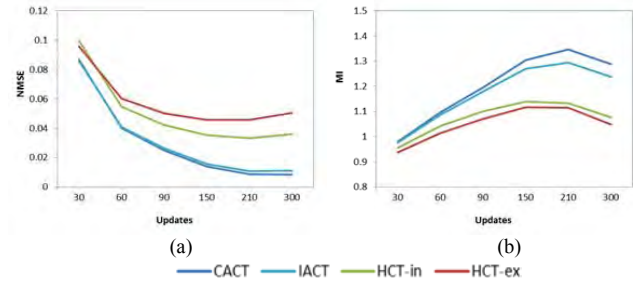


Fig. 5 (a) NMSE and (b) MI results for phantom with no thoracic lesion and with respiratory motion amplitude of 2 cm.

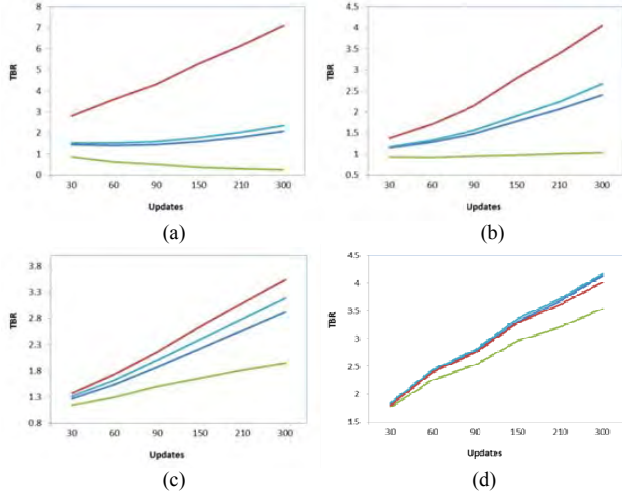


Fig. 6 The TBR results for 20 mm lesion located at (a) LLL (b) LRL (c) MRL and (d) URL. The standard TBR was 4:1 and respiratory amplitude was 2 cm.

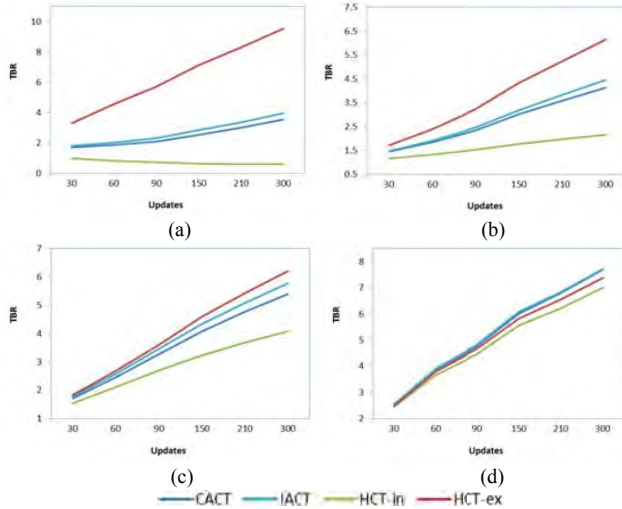


Fig. 7 The TBR results for 20 mm lesion located at (a) LLL (b) LRL (c) MRL and (d) URL. The standard TBR was 8:1 and respiratory amplitude was 2 cm.

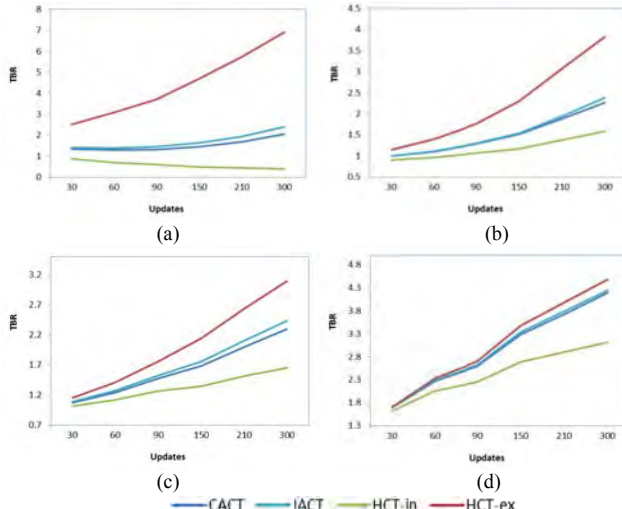


Fig. 8. The TBR results for 10 mm lesion located at (a) LLL (b) LRL (c) MRL and (d) URL. The standard TBR was 8:1 and respiratory amplitude was 2 cm.

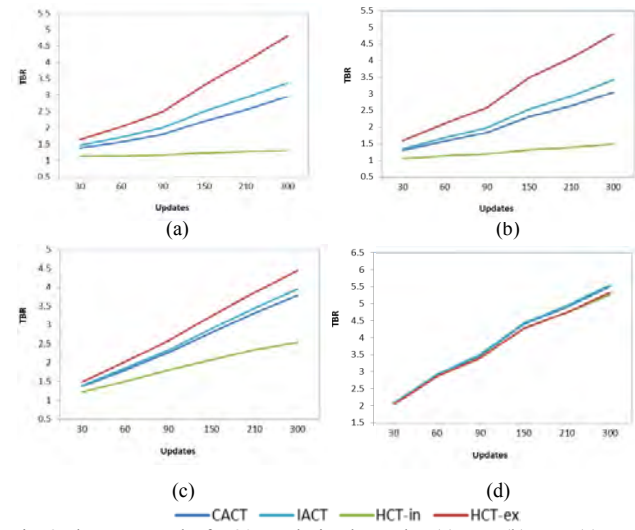


Fig. 9 The TBR results for 20 mm lesion located at (a) LLL (b) LRL (c) MRL and (d) URL for a standard TBR of 6:1 and respiratory amplitude of 3 cm.

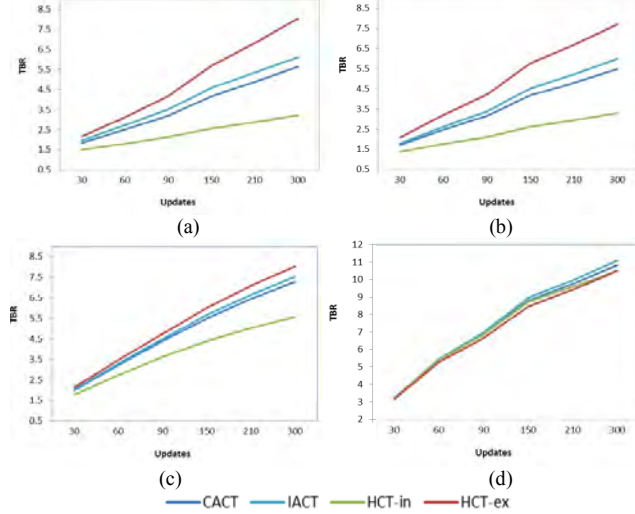


Fig. 10 The TBR results for 20 mm lesion located at (a) LLL (b) LRL (c) MRL and (d) URL with standard TBR of 12:1 and respiratory amplitude of 3 cm.

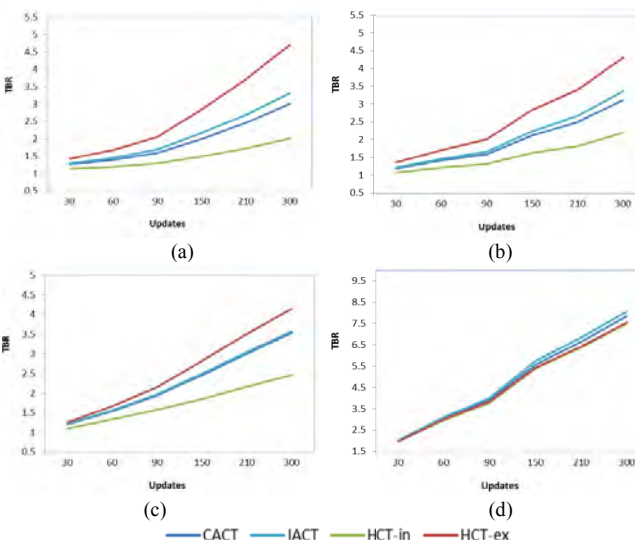


Fig. 11 The TBR results for 10 mm lesion located at (a) LLL (b) LRL (c) MRL and (d) URL for a standard TBR of 12:1 and respiratory amplitude of 3 cm.

IV. CONCLUSION

In conclusion, the global reconstructed image quality was superior for PET_{CACT}/PET_{IACT}. For local lesion detection, PET_{IACT} more closely mimicked PET_{CACT} for all simulated lesion locations, uptake ratios and sizes, while PET_{HCT-in} consistently showed under-estimation and the performance of PET_{HCT-ex} depended on the location. The PET_{HCT} deviated from PET_{CACT}/PET_{IACT} more for the lower level lesions, following by the middle level and upper level lesions. The TBRs of 10 mm lesions were more difficult to be recovered for all AC maps. IACT works similarly for different lesion sizes and uptake ratios. Better lesion localization, more stable quantitation and lower dose of IACT for different lesion characteristics and respiratory motion amplitudes make it a good alternate for AC as compared to conventional HCT/CACT, especially in further oncology treatment planning.

V. REFERENCES

- [1] Mok GSP, Sun T, Huang TC and Vai MI, "Interpolated average CT for attenuation correction in PET - a simulation study", *IEEE Trans Biomed Eng.* 2013 Jul; 60(7):1927-34.
- [2] Sun T, Wu TH, Wang SJ, Yang BH, Wu NY and Mok GSP, "Low dose interpolated average CT for PET/CT attenuation correction using an active breathing controller", *Med. Phys.* 2013 Oct; 40(10):102507.
- [3] Huang TC, Mok GSP, Wang SJ, Wu TH and Zhang G, "Attenuation correction of PET images with interpolated average CT for thoracic tumors", *Phys. Med. Biol.*, vol. 56, pp. 2559-2567, 2011.